

Variability in strontium and lithium concentration of ancient seawater from fluid inclusions in halite—implications for reconstructing drivers of seawater secular variability

EGU General Assembly 2024

drivers of seawater secular variability



Mebrahtu F. Weldeghebriel (mweldeg@princeton.edu)^{1,2},

Tim K. Lowenstein², John A. Higgins¹

¹Department of Geosciences, Princeton University, Princeton, USA, ²Department of Earth Sciences, Binghamton University, Binghamton,

ABSTRACT

Secular variations in the major ion chemistry and isotopic composition of seawater on multimillion-year time scales over the Phanerozoic are well documented, but the causes of these changes are debated. $\delta^7\text{Li}$ and $^{87}\text{Sr}/^{86}\text{Sr}$ are widely utilized to interpret the driving mechanisms of secular changes in seawater chemistry, the tectonic history of the Earth and the link between paleo-ocean chemistry and the carbon cycle. These interpretations and models, however, are based on (1) few quantitative data on strontium concentration $[\text{Sr}]_{\text{SW}}$ in seawater calculated from the Sr/Ca ratios of marine carbonates and (2) the assumption that the Li concentration $[\text{Li}]_{\text{SW}}$ of seawater has been similar to modern $[\text{Li}]_{\text{SW}}$. But those assumptions, if inaccurate, could undermine the validity of modeling results. The marine strontium and lithium cycles through time could be better reconstructed using coupled marine records of $[\text{Sr}]_{\text{SW}}$, $^{87}\text{Sr}/^{86}\text{Sr}$, $[\text{Li}]_{\text{SW}}$ and $\delta^7\text{Li}$. $[\text{Sr}]_{\text{SW}}$ and $[\text{Li}]_{\text{SW}}$ in ancient seawater would be particularly useful for examining which global processes, continental weathering, marine reverse weathering or global volcanicity at seafloor hydrothermal systems and subduction zones, exerted the dominant control on the changes in seawater chemistry. Recent analytical advances using combined cryo-SEM-EDS and laser ablation ICP-MS now allow quantitative measurement of $[\text{Sr}]_{\text{FI}}$ and $[\text{Li}]_{\text{FI}}$ in fluid inclusions in halite. $[\text{Sr}]_{\text{SW}}$ and $[\text{Li}]_{\text{SW}}$, reconstructed from chemical analyses of >1,000 fluid inclusions in more than 100 halite samples with marine $^{87}\text{Sr}/^{86}\text{Sr}$ values, varied seven-ten-fold and oscillated twice between high- and low-Sr and Li concentrations over the past 550 million years, in rhythm with Ca-rich and SO_4 -poor paleoseawater intervals, calcite-aragonite seas, supercontinent breakup, dispersal, and assembly cycles, greenhouse-icehouse climates, and modeled atmospheric $p\text{CO}_2$. These data enable us to better constrain the Sr and Li cycle, and offer new insights into geochemical modeling of Phanerozoic seawater chemistry using multiple isotope systems and seawater concentrations.

METHODS

LA-ICP-MS was used to determine the Sr, Li, Ca, and Mg concentrations of fluid inclusions in marine halite (Weldeghebriel et al., 2020). We selected 131 halite samples from Neoproterozoic and Phanerozoic evaporite basins with previously measured $^{87}\text{Sr}/^{86}\text{Sr}$ ratios of marine origin (Weldeghebriel et al., 2022).

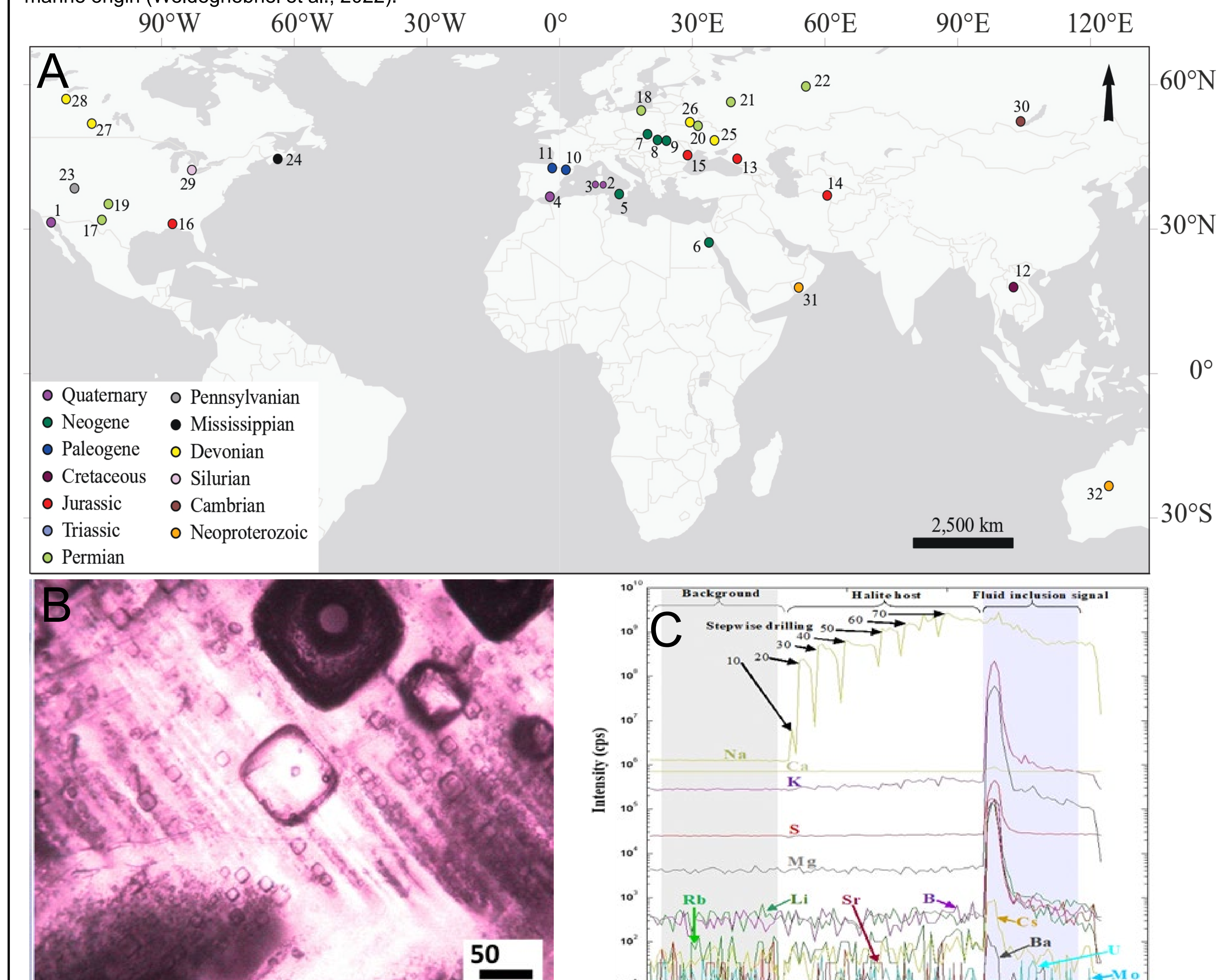


Fig 1. (A) Map showing global distribution of marine evaporite basins used in this study. Numbers on the map refer to the 32 evaporite basins. (B) 80 μm primary fluid inclusion in the center parallel to growth zones in chevron crystal. Fluid inclusion at the top with dark area has ablation crater produced by the laser beam during analysis. (C) LA-ICP-MS time-resolved spectrum showing transient signal intensities and stepwise ablation technique during analysis of fluid inclusions in halite. The Sr, Li, Ca, and Mg signals increased exponentially from the background values when the laser beam breached the fluid inclusion at ~165 sec.

RESULTS

$[\text{Sr}]_{\text{SW}}$ and $[\text{Li}]_{\text{SW}}$ varied seven and twelve-fold, respectively, and oscillated twice between high- and low- Sr and Li concentrations since 550 Ma, in rhythm with $[\text{Ca}^{2+}]_{\text{SW}}$, $\text{Mg}/\text{Ca}_{\text{SW}}$, atmospheric $p\text{CO}_2$, aragonite-calcite-seas, $\text{KCl}-\text{MgSO}_4$ evaporites, greenhouse-icehouse climates, and supercontinent assembly and dispersal cycle (Fig. 2).

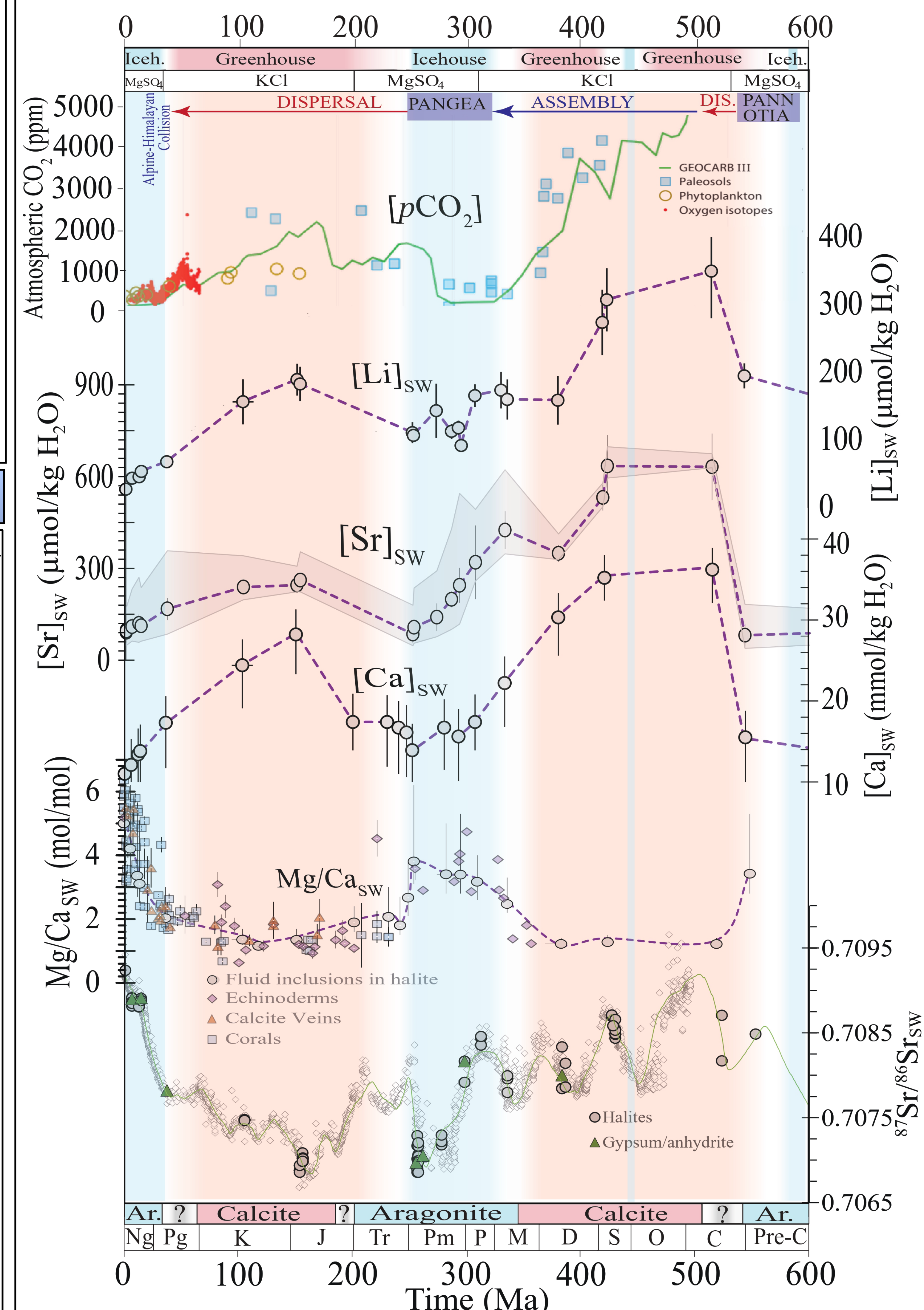


Fig 2. Secular variation in Phanerozoic and Neoproterozoic seawater $[\text{Li}]_{\text{SW}}$ (Weldeghebriel and Lowenstein, 2023), $[\text{Sr}]_{\text{SW}}$ (Weldeghebriel et al., 2023), $[\text{Ca}]_{\text{SW}}$ (Weldeghebriel et al., 2022 and references therein), $\text{Mg}/\text{Ca}_{\text{SW}}$ ratios (Coggon et al., 2010; Dickson et al., 2002; Gothmann et al., 2015; Weldeghebriel et al., 2022 and references therein), and $^{87}\text{Sr}/^{86}\text{Sr}_{\text{SW}}$ (Prokoph et al., 2008). Gray circles show $[\text{Li}]_{\text{SW}}$, $[\text{Sr}]_{\text{SW}}$, $[\text{Ca}]_{\text{SW}}$, $\text{Mg}/\text{Ca}_{\text{SW}}$, and $^{87}\text{Sr}/^{86}\text{Sr}$ values from fluid inclusions in marine halite with 1 SD (2SE for $^{87}\text{Sr}/^{86}\text{Sr}_{\text{SW}}$) error bars, green triangles show $^{87}\text{Sr}/^{86}\text{Sr}$ values in sulfates interbedded with halite, $\text{Mg}/\text{Ca}_{\text{SW}}$ ratios from echinoderm (diamond), calcite veins (triangle), and corals (square). Phanerozoic atmospheric CO_2 concentrations, modified from Turchyn and DePablo, 2019. Supercontinent cycle (dispersal, assembly) from Frizon De Lamotte et al. (2015) and Kroner et al. (2021). Blue and pink shading show greenhouse-icehouse climates (McKenzie et al., 2016). Horizontal bars at the top and bottom of the figure are $\text{MgSO}_4\text{-KCl}$ potash evaporites (Hardie, 1996), and aragonite-calcite seas (Sandberg, 1983).

DISCUSSION

$[\text{Sr}]_{\text{SW}}$ and $^{87}\text{Sr}/^{86}\text{Sr}$ (~500–250 Ma) coincides with the assembly of the supercontinent Pangaea in the Paleozoic, and from ~150–0 Ma, matches the break-up of Pangaea in the Mesozoic and Cenozoic (Fig. 3A). The $^{87}\text{Sr}/^{86}\text{Sr}$ and $[\text{Sr}]_{\text{SW}}$ trends may be linked to supercontinent cycles (Weldeghebriel et al., 2023). The strong positive correlation between $[\text{Sr}]_{\text{SW}}$ and $[\text{Li}]_{\text{SW}}$ over the Phanerozoic have implications for interpreting the secular evolution of major ion composition of seawater. Li is entirely derived from terrestrial silicate mineral weathering and seafloor-basalt interactions with hydrothermal fluids at MORs, and its concentration in seawater is not significantly influenced by biological processes or precipitation of carbonates. However, marine carbonate deposition constitutes the major global sink of Sr in the oceans, and Sr concentration in seawater is strongly influenced by the primary carbonate mineralogy (aragonite vs. calcite).

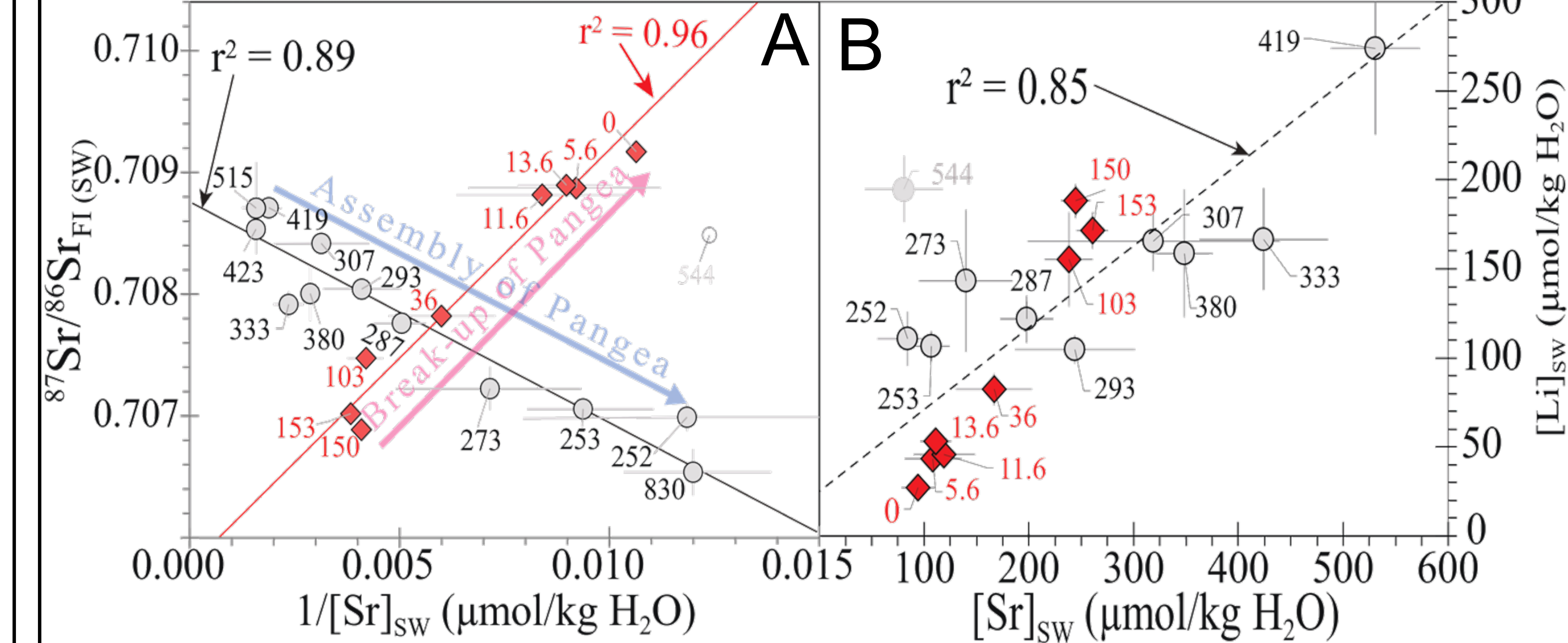


Fig 3. Covariations between $^{87}\text{Sr}/^{86}\text{Sr}$ ratio, $[\text{Sr}]_{\text{SW}}$, and $[\text{Li}]_{\text{SW}}$ from fluid inclusions in Phanerozoic and Neoproterozoic marine. (A) Two linear regression curves show relationship between $[\text{Sr}]_{\text{SW}}$ and $^{87}\text{Sr}/^{86}\text{Sr}$ from 0–150 Ma (red) and 252–830 Ma (black) (Weldeghebriel et al., 2023). Assembly and break-up processes of Pangaea are indicated by arrows (Cawood and Buchan, 2007). The $^{87}\text{Sr}/^{86}\text{Sr}$ ratio versus $1/[\text{Sr}]_{\text{SW}}$ during the final assembly of Pangaea in the Permian (ca. 252 Ma) plots near the final stages of assembly of Rodinia in the Cryogenian (ca. 825 Ma) (Li et al., 2008). Ages in million years adjacent to the symbols. (B) Covariation of $[\text{Li}]_{\text{SW}}$ with $[\text{Sr}]_{\text{SW}}$ from fluid inclusions. Phanerozoic and Neoproterozoic marine halite. Linear regression curve show relationship between $[\text{Li}]_{\text{SW}}$ and $[\text{Sr}]_{\text{SW}}$ from 0–150 Ma (red) and 252–830 Ma (black).

SUMMARY AND FUTURE WORK

- Fluid inclusions in marine halite record the $[\text{Sr}]_{\text{SW}}$ and $[\text{Li}]_{\text{SW}}$ of the Neoproterozoic and Phanerozoic seawater.
- $[\text{Sr}]_{\text{SW}}$ and $[\text{Li}]_{\text{SW}}$ varied in rhythm with the major ion composition of Phanerozoic seawater, icehouse-greenhouse climate, and supercontinent cycle.
- Coupled marine records of $[\text{Sr}]_{\text{SW}}$, $^{87}\text{Sr}/^{86}\text{Sr}$, $[\text{Li}]_{\text{SW}}$ and $\delta^7\text{Li}$ provide additional constrains for future modeling of changes in ancient seawater chemistry.



REFERENCES

Cawood and Buchan (2007) Earth Sci. Rev. 82, 217–256.
 Coggon et. Al (2010) Science 327, 1114–1117.
 Dickson (2002) Science 298, 1222–1224.
 Frizon De Lamotte et al. (2015) Tectonics 34, 1009–1029.
 Hardie (1996) Geology 24: 279–283.
 Gothmann et al. (2015) Geochim. Cosmochim. Acta 160, 188–208.
 Kroner (2021) Geol. Soc. Spec. Publ. 503, 83–104.
 Li et al. (2008) Precambrian Res. 160, 179–210.
 McKenzie et al. (2016) Science 352, 444–447.
 Prokoph et al. (2008) Earth Sci. Rev. 87, 113–133.
 Sandberg (1983) Nature 305:19–22.
 Turchyn and DePaolo (2019) Annu. Rev. Earth Planet. Sci. 47, 197–224.
 Weldeghebriel et al. (2020) Chem. Geol. 551, 119762.
 Weldeghebriel et al. (2022) Earth Planet. Sci. Lett. 594, 117712.
 Weldeghebriel et al. (2023) Geochim. Cosmochim. Acta 346, 165–179.
 Weldeghebriel and Lowenstein (2023) Sci. Adv. 9, eadf1605.